Magnetic and Kinetic Power Spectra as a Tool to Probe the Turbulent Dynamo

V. Abramenko, V. Yurchyshyn, and P.R. Goode

Big Bear Solar Observatory of New Jersey Institute of Technology, 40386, North Shore Ln,

Big Bear City, CA, USA

ABSTRACT

Generation and diffusion of the magnetic field on the Sun is a key mechanism responsible for solar activity on all spatial and temporal scales - from the solar cycle down to the evolution of small-scale magnetic elements in the quiet Sun. The solar dynamo operates as a non-linear dynamical process and is thought to be manifest in two types: as a global dynamo responsible for the solar cycle periodicity, and as a small-scale turbulent dynamo responsible for the formation of magnetic carpet in the quiet Sun. Numerous MHD simulations of the solar turbulence did not yet reach a consensus as to the existence of a turbulent dynamo on the Sun. At the same time, high-resolution observations of the quiet Sun from Hinode instruments suggest possibilities for the turbulent dynamo. Analysis of characteristics of turbulence derived from observations would be beneficial in tackling the problem. We analyze magnetic and velocity energy spectra as derived from Hinode/SOT, SOHO/MDI, SDO/HMI and the New Solar Telescope (NST) of Big Bear Solar Observatory (BBSO) to explore the possibilities for the small-scale turbulent dynamo in the quiet Sun.

1. Introduction

A dynamo process can be defined as the generation of the magnetic field from an inverse cascade due to motions in a conducting medium. In the convective envelope of the Sun, such motions are the result of turbulent convection in the photosphere and beneath. The turbulent character of these motions is clearly demonstrated by observations. As an example we present high-resolution observations (Figure 1) of quiet sun (QS) granulation obtained recently with the 1.6 meter New Solar telescope (NST) of Big Bear Solar Observatory (BBSO, Goode et al. 2010a,b). The corresponding two-hour movie is available at the BBSO website `http://bbso.njit.edu/gallery/nst_tio_20100803.mpg`. Statistical analysis of this data set can be found in Abramenko et al. (2010, 2011) and at `http://www.bbso.njit.edu/~avi/2011NSF/`.
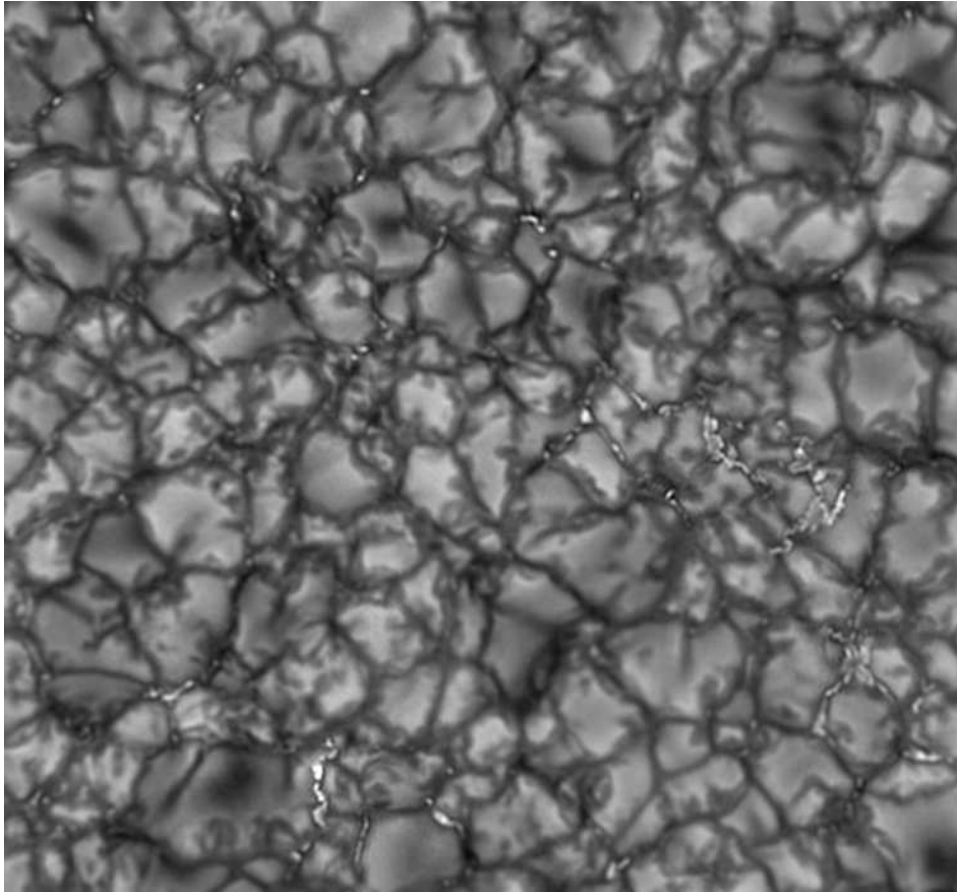
Fig. 1.— Image of solar granulation in a quiet sun area observed on August 3, 2010 at 17:06 UT with the NST of BBSO equipped with a TiO filter. The pixel size is 0.0375 ″ and the size of the image is 28.3 × 26.2 ″. A movie of the corresponding 2-hour data set further illustrates the turbulent nature of solar plasma flows in the photosphere (see the text for the link).

Turbulent dynamo operation implies a gradual gain of magnetic energy inside a volume (Batchelor 1950, Kazantsev 1968). Numerical simulations allow one to probe the turbulent dynamo action (e.g., Boldyrev 2001, Schekochihin et al. 2002, Cho et al. 2003, Boldyrev & Cattaneo 2004). Indeed, fron an initial moment for a simulation, one may track the evolution of the magnetic energy accumulated in the volume. In the case an increase of magnetic energy is detected, one can argue for a dynamo action. Unfortunately, this is not a possibility when one deals with observational data. There is no apparent moment of initiation, and the magnetic energy is constantly generated and dissipated keeping the plasma in a state of dynamical equilibrium. We have to find some approach to test this turbulent state and to make inferences on the possibilities of turbulent dynamo action.

Two approaches might be suggested. First, one may test the interplay between the kinetic and magnetic energies, i.e., to explore the spatial power spectra of kinetic and magnetic energy. Second, one might test the structural organization of the magnetic and velocity fields in QS, namely, to explore their multifractal properties. Let us consider a theoretical background for the first approach.
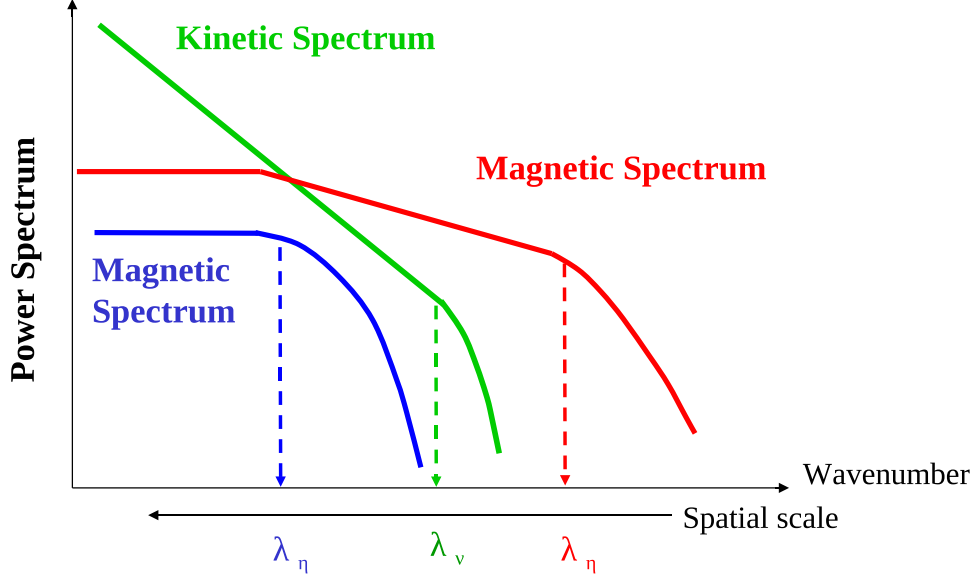

Fig. 2.— Sketch of a mutual behavior of the kinetic and magnetic power spectra in a turbulent medium. Red and green lines: - a case of high Prandtl number ($Pr = \lambda_\nu/\lambda_\eta$) when the magnetic spectrum is more shallow than the velocity spectrum, and at scales larger than λ_ν, the magnetic energy dominates the kinetic energy. In this limit, the situation is favorable for turbulent dynamo action. Blue and green lines: - a case of low Prandtl number, when the magnetic spectrum shows a dissipation cut-off at scales much larger than λ_ν, magnetic eddies are exhausted at smaller scales, and the dynamo action is questionable.

In Figure 2, the green line schematically represents a spatial power spectrum of the turbulent velocities in the QS photosphere. The kinetic energy, being deposited at large scales via the large-scale convective subphotospheric motions, cascades down to smaller scales, producing the Kolmogorov-type spectrum of -5/3. At some scale, λ_ν, the kinetic vorticies start to dissipate, which results as a cut-off of the spectrum.

In order to generate magnetic fields at a scale λ, the following condition should be met: the characteristic time for the curling of a magnetic field line by a plasma's vortex (of size λ) should be shorter than the characteristic time for the dissipation of a magnetic vortex of the same size. This further requires that the Prandtl number - the ratio of the kinetic dissipation scale to the magnetic dissipation scale, λ_ν/λ_η, - has to exceed unity (Pikelner

1961, Biskamp 1993). At a high Prandtl number the small-scale turbulent dynamo action is both proved theoretically and in simulations (Batchelor 1950, Nakagawa & Priest 1973, Boldyrev 2001, Schekochihin et al. 2002, Cho et al. 2003). In this case, the magnetic spectrum (red line in Figure 2) is shallower than the kinetic one (green line in Figure 2), so that magnetic dissipation starts at scales, λ_η, much smaller than that for the kinetic dissipation scale.

For the opposite case of low Prandtl number (blue line in Figure 2), the magnetic dissipation starts on much larger scales, $\lambda_\eta > \lambda_\nu$. Here, the turbulent dynamo action is very problematic, at least, at very small scales ($\lambda < \lambda_\eta$) because these small magnetic eddies cannot survive. However, there are studies aimed at probing the turbulent dynamo at low Prandtl number via numerical simulations (see, e.g., Boldyrev & Cattaneo 2004, Iskakov et al. 2007, Pietarila Graham et al. 2010).

Thus, it is useful to see how the real kinetic and magnetic spectra behave in the QS photosphere.

2.   Kinetic and Magnetic Energy Spectra

To obtain the magnetic and kinetic energy spectra in the QS photosphere, we utilized 2D images of the magnetic and velocity field components. From a squared 2D Fourier transform of an image, we calculated the angle-integrated 1D power spectra. The routine is described in details in Abramenko et al. (2001), Abramenko (2005a).

For a comprehensive analysis, we explore how the magnetic and kinetic spectra vary as the resolution of instruments improves. For that, we augmented our own calculations of the spectra by those published in the past, when the available spatial resolution was poor. Assuming a uniform spatial distribution of the mass at any depth, we consider the power spectrum of the velocity field components to be a representative of the kinetic energy spectrum.

Figure 3 shows magnetic and velocity spectra as derived from observations. In the lower left panel, three velocity spectra for QS areas are shown:

- a Doppler velocity spectrum from Peak du Midi observations with resolution of $0.8''$ (Espagnet et al. (1993), blue line);

- a Doppler velocity spectrum from Hinode/SOT observations in the spectral line 6301Å recorded on March 10, 2008 (red line), the pixel size of $0.16''$;

- a transverse velocity spectrum from NST observations of the solar granulation obtained from the data presented in Figure 1. The transverse velocity field components, V_x and V_y, were computed via a local correlation tracking (LCT) technique (Strous 1996, Abramenko et al. 2008). The FWHM of the Gaussian tracking window was 10×10 pixels ($0.375''$). To obtain one velocity map, an averaging over 12 time-steps (2 minutes) was undertaken. Total, 54 flow maps of 342×342 nodal points each were computed. Angle-integrated power spectra (Abramenko 2005a) from each V_x, V_y map were calculated and then averaged over 54 maps. Resulting spectra of V_x and V_y are shown in the lower panels of Figure 3.

All the spectra show a smooth transition to the Kolmogorov-type regime with a slope of -5/3 at scales of about 1.5-3 Mm. No well-pronounced tendency following the improvement in the spatial resolution is observed.

Magnetic energy spectra obtained from observations are shown in the top panels of Figure 3. The top left panel shows spectra obtained from Hinode/SOT/SP data of a QS area observed on 2007 Mar 10. The spectrum derived from the inversion technique (blue line, the LOS-flux spectrum) is very similar in shape to the spectrum of B_{app}^L (red line) derived from the Stokes profiles intensities (Lites et al. 2008), however the LOS-flux spectrum possesses more magnetic power at each scale. This means that the power distribution along the spectrum and, therefore, the magnetic structuring, are captured equally by both techniques. The difference in power arises from the LOS-flux values being systematically higher. The spectrum of the transverse component, B_{app}^T (purple line), shows a presence of noise at small scales (a positive slope range at smallest scales), which is not the case for the longitudinal component spectra. The specific energy stored in the transverse component appears to be lower than that in the longitudinal component. The most important point here is that the transverse spectrum extends its shallow slope further toward small scales than the longitudinal spectrum does. This means that the turbulent dynamo action is better manifested in the transverse field generation.

Gradual improvements in our knowledge of magnetic power spectra occur with the improvement of spatial resolution of solar instrumentation, and are illustrated in the top right panel of Figure 3, where we plot together many published and computed spectra (all spectra are shifted along the vertical axis). Peak du Midi data (Nakagawa & Priest 1973) with $5''$ resolution (black line) show a smooth cut-off at scales about 20 Mm. MDI full disk data (green line) of $2''$ resolution demonstrate a cut-off at about 10 Mm. The steeper slope below 10 Mm might be an energy cascade signature, however, observations with higher spatial resolution (dark blue line, HMI data) demonstrate an extension of the shallow magnetic spectra toward smaller scales, down to 4-5 Mm. Observations with Hinode/SOT

further show that the magnetic spectrum extends with approximately the same slope (of about -1/3) down to 1 Mm scale. This behavior is essentially different from that we saw for the velocity spectra. We may speculate that future observations with better resolution will allow us to obtain even more extended shallow magnetic spectrum, in accordance with the thin straight line in the top right panel of Figure 3. Compared to the velocity spectrum (bottom right panel in Figure 3), the slope and the extend of the thin line may ensure a possibility for prevalence of magnetic energy over the kinetic energy at small scales, below approximately $\lambda_{TD} \approx 1 - 0.5$ Mm, and therefore, a possibility for turbulent dynamo action. Note that the position of the kinetic spectrum relative to the vertical axis strongly depends on the magnitude of the photospheric plasma density. Here we accepted its value as 10^{-7} g cm^{-3}. Further studies of photospheric plasma's conditions may bring some corrections in the position of the kinetic spectrum, and, therefore, in λ_{TD}.

3. Intermittency and Multifractality Spectra of the Magnetic Field

The multifractal organization of the magnetic field means that random strong peaks in the vector field transport by a random flow (say, the magnetic field vector in a turbulent electro-conductive flow) correspond to structural features such as magnetic flux ropes or thin sheets of magnetic field lines. Thus, a weak seed magnetic field may grow exponentially, a phenomenon known as a turbulent dynamo. The presence of multifractality is physically compatible with turbulent dynamo action. The property of multifractality is also frequently referred to as intermittency (see, e.g., Abramenko (2008) for a review of intermittency and multifractality in solar phenomena). Numerical simulations (Cho et al. 2002) of the MHD turbulence at high Prandtl number demonstrate highly intermittent magnetic field organization. Simulations of turbulent magnetic reconnection (Matthaeus & Lamkin 1986) show that magnetically dominated modes (in the kinetic and magnetic spectra) correspond to strong peaks in both magnetic and velocity fields.

Observations from Hinode show that the photospheric magnetic field in QS is intermittent: the blue line in the left panel of Figure 4 is a flatness function (for definition, see, e.g., Frisch 1995, Abramenko 2005b, Abramenko & Yurchyshyn 2010) which we calculated from Hinode/SOT/SP LOS magnetic flux map of a QS area observed on February 3, 2008. At small scales (less than 4 Mm), the function increases as the scale decreases, which means a multifractal organization and intermittency of the magnetic field. For comparison, in the same figure we show a flatness function (green line) calculated for a typical active region (AR) from observations with lower resolution. Intermittency in the magnetic field is also present, however, at much larger scales (2-30 Mm).

A widely accepted metric to characterize multifractality is the spectrum of multifractality, $f(\alpha)$ (see, e.g., Feder 1989, Lawrence et al. 1993, Schroeder 2000, Conlon et al. 2008, McAteer et al. 2010). Black line in the right panel of Figure 4 represents a spectrum of multifractality, which we derived from the Hinode/SOT/SP LOS magnetic flux map of a QS area observed on February 3, 2008. We see that a broad range of the scaling exponent α is allowed, and for each α, according to definition, there exists a sub-set, i.e., a monofractal, of the fractal dimension $f(\alpha)$, so that all of them being superposed, create a resulting observed magnetic multifractal. Behavior of the QS multifractality spectrum is similar to that observed for strong-flaring ARs (see the right panel of Figure 4). This implies similar multifractal organization of the magnetic field, but in the case of the QS it occurs at much smaller spatial scales.

4. Summary

New generation solar instruments, namely, Hinode/SOT/SP and BBSO/NST demonstrate previously unclear tendencies in the behavior of QS magnetic and velocity fields.

First, as the resolution improves, the shallow magnetic energy spectrum tends to extend toward higher wave-numbers (smaller scales), the slope remaining the same, whereas the velocity spectrum shows a steady maximum at 1-3 Mm followed by the Kolmogorov-type regime of $E(k) \sim k^{-5/3}$. This tendency necessarily results in setting in high-Prandtl number turbulence with necessary turbulent dynamo action at small scales below $\lambda_{TD} \approx 1 - 0.5$ Mm.

Second, improved resolution of solar data revealed a highly intermittent and multifractal nature of the small-scale magnetic field in QS areas. This property of the magnetic field is extremely favorable for the turbulent dynamo action at all scales where the intermittency/multifractality is present.

REFERENCES

Abramenko, V., Yurchyshyn, V., Wang, H., Goode, P. R. 2001, Solar Phys., 2001, 225

Abramenko, V. I. 2005a, ApJ, 629, 1141

Abramenko, V. I. 2005b, Solar Phys., 228, 29

Abramenko, V. I. 2008, in: :Solar Physics Research Trends",ed. Pingzhi Wang, Nova Science Publishers, Inc., New York, pp 95-136

Abramenko, V., Yurchyshyn, V., Wang, H. 2008, ApJ, 681, 1669

Abramenko, V., Yurchyshyn, V., 2010, ApJ, 722, 122

Abramenko, V., Yurchyshyn, V., Goode, P.R., Kilcik, A. 2010, ApJ, 725, L1.

Abramenko, V. I., Carbone, V., Yurchyshyn, V., Goode, P. R., Stein, R. F., Lepreti, F., Capparelli, V., Vecchio, A. 2011, ApL, 743, 133

Batchelor, G. K. 1950, Proceedings of the Royal Society of London. Series A, Mathematical and Physical Sciences, Volume 201, Issue 1066, pp. 405-416

Biskamp, D., 1993, "Nonlinear Magnetohydrodynamics", eds.: W. Grossman, D. Papadopoulos, R. Sagdeev and K. Schlindler, Cambridge University Press, Cabmridge, New York, Melbourne, 378 pp

Boldyrev, S., 2001, ApJ, 562, 1081

Boldyrev, S., Cattaneo, F. 2004, Phys. Rev. Lett., 92, 144501

Cho,J., Lazarian, A., Vishniac, E.T. 2003, ApJ, 595, 812

Conlon, P.A., Gallagher, P.T., McAteer, R.T.J., Ireland, J., Young, C.A., Kestener, P., Hewett, R.J., Maguire, K. 2008, Solar Phys., 248, 297

Espagnet, O., Muller, R., Roudier, T., Mein, N., 1993, Astron. Astrophys., 271, 589

Feder, J. 1989, "Fractals", Plenum Press, New York and London

Frisch, U. "Turbulence, The Legacy of A.N. Kolmogorov", Cambridge University Press, 1995

Goode, P. R., Coulter, R., Gorceix, N., Yurchyshyn, V., Cao, W. 2010a, Astronomische Nachrichten, 331, 620

Goode, P. R., Yurchyshyn, V., Cao, W., Abramenko, V., Andic,A., Ahn, K., Chae, J., 2010b, ApJ, 714, L31

Iskakov, A.B., Schekochihin, A.A., Cowley, S.C., McWilliams, J.C., Proctor, M.R.E. 2007, Physical Review Letters, 98, 208501

Kazantsev, A.P., 1968, Soviet Phys. - JETP, 26, 1031

Lawrence, J.K., Ruzmaikin, A.A., Cadavid, A.C. 1993, ApJ, 417, 805

Lites, B. W., Kubo, M., Socas-Navarro, H., and 11 co-authors, 2008, ApJ, 672, 1237

Matthaeus, W.H., Lamkin, S.L. 1986, Physics of Fluids, 29, 2513

McAteer,R.T.J.,Gallagher, P.T., Conlon, P.A. 2010, Advances in Space Research, 45,1067

Nakagawa, Y., Priest, E.R., 1973, ApJ, 179, 949

Parnell, C. E., DeForest, C. E., Hagenaar, H. J., Johnston, B. A., Lamb, D. A., Welsch, B. T. 2009, ApJ, 698, 75

Pietarila Graham, J., Danilovic, S., Schuessler, M. 2010, ArXiv e-prints, http://adsabs.harvard.edu/abs/2010arXiv1003.0347P

Pikel'ner, S.B. 1961, "Fundamentals of Cosmic Electrodynamics", ed. by B.E. Gelfgat, Moscow, 295 pp

Schekochihin, A.A., Boldyrev,S.A., Kulsrud,R.M. 2002, ApJ, 567, 828

Schroeder, M. 2000, "Fractals, Chaos, Power Laws: Minutes from an Infinite Paradise", W.H.Freeman and Company, New York

Strous, L. H., Scharmer, G., Tarbell, T. D., Title, A. M., Zwaan, C. 1996, Astron Astrophys., 306, 947
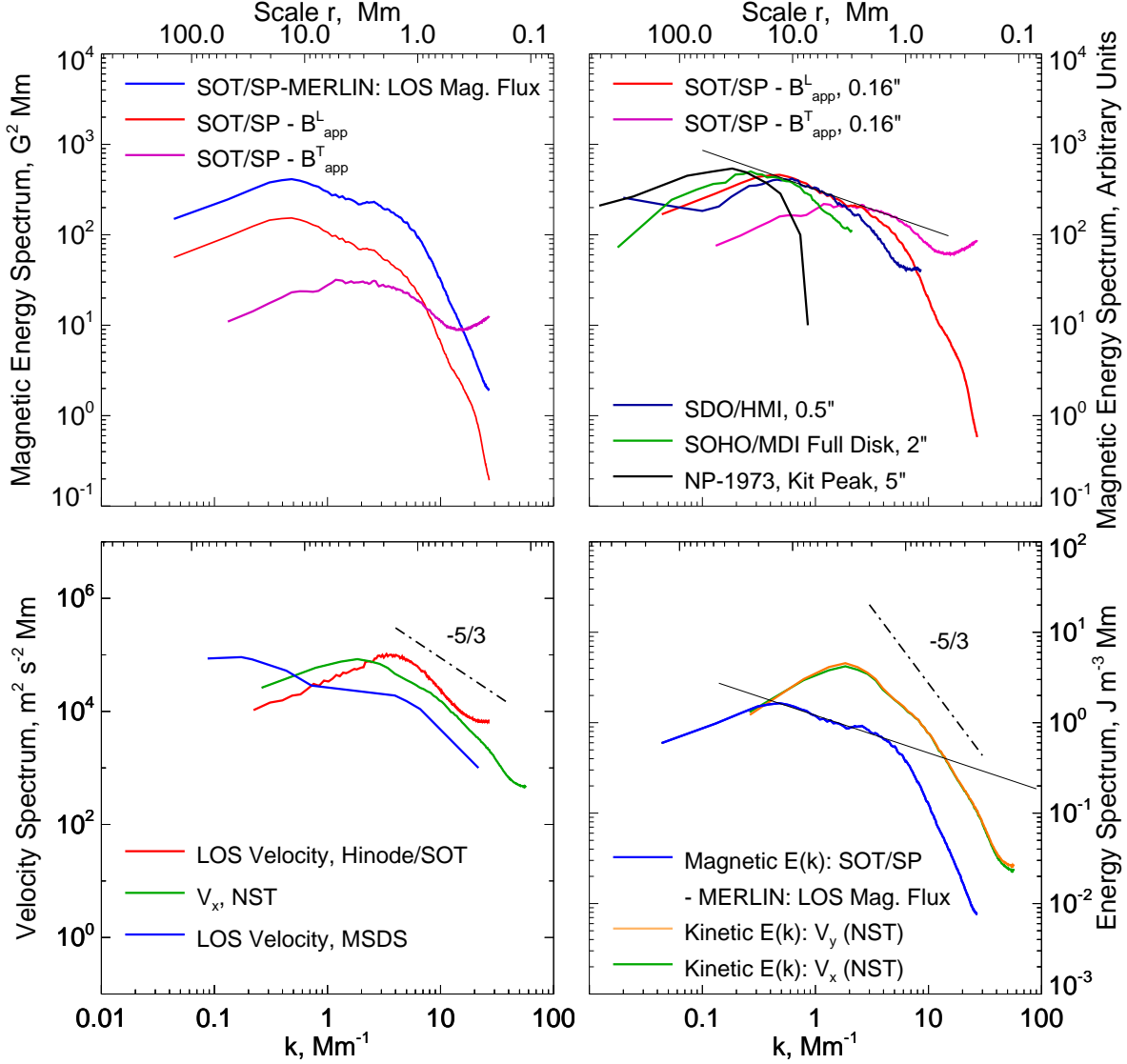
Fig. 3.— Magnetic and kinetic energy spectra from QS measurements. Top left panel: magnetic spectra from Hinode/SOT/SP instrument (Tsuneta et al. 2008) recorded on 2007 March 10 at 11:37 UT. Top right: magnetic spectra derived from observations with different instruments. The pixel size of each data set is noted. For better comparison, the spectra are shifted along the vertical axis. Black line: Nakagawa $ Priest (1973) spectrum. As the resolution improves, the cut-off of the spectra occurs at higher wave-numbers. The thin straight line shows a tentative behavior of the spectra when the resolution is better than 0.16″. Bottom left: Velocity spectra. Blue line: Peak du Midi observations of Doppler velocities with resolution of 0.8″ (Espagnet et al. 1993; this spectrum was shifted along the vertical axis). Red line: Doppler velocities from Hinode SOT/SP. Green line: a spectrum of the V_x component of the transverse velocities calculated from the NST data set presented in Figure 1. Bottom right: kinetic energy spectra over-plotted with a magnetic energy spectrum. Thin black line is a best linear fit to the magnetic spectrum above a cutoff. The Kolmogorov-type spectrum (-5/3) is shown with the dash-dot lines.
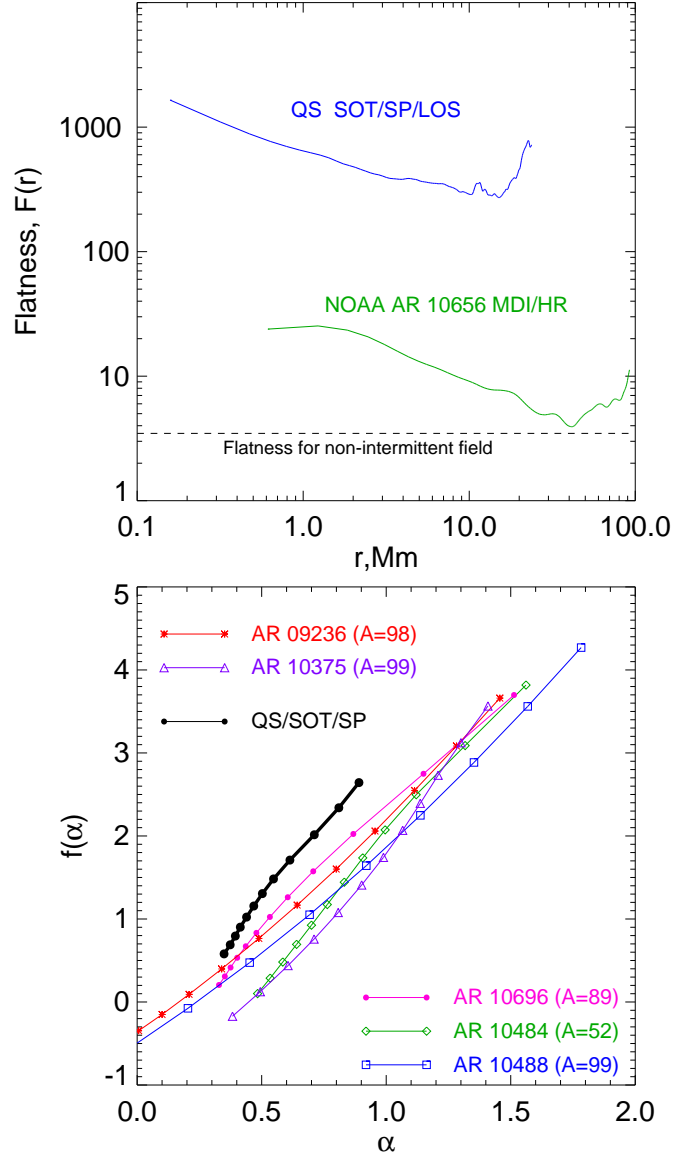
Fig. 4.— Top: Flatness functions of the LOS magnetic fields measured for a typical QS area observed with Hinode/SOT/SP with a pixel size of 0.16″ and for a typical AR (SOHO/MDI high resolution data, pixel size of 0.6″) Flatness function is flat (dashed line) for a non-intermittent, monofractal, non-flaring structure, and it becomes steeper with decreasing spatial scales for intermittent fields. The steeper the function, the more complex the fields are. Bottom: Multifractality spectra $f(\alpha)$ calculated for the same QS area and for five ARs of high flaring activity (the flare index, A, proportional to the flare productivity of an AR, is shown, Abramenko & Yurchyshyn 2010).